

Review

Corrosion resistance of Fe-Cr-based amorphous alloys: An overview

C.A.C. Souza^{a,*}, D.V. Ribeiro^a, C.S. Kiminami^b^a Department of Materials Science and Technology, Federal University of Bahia, Rua Aristides Novis, 02 Federação, 40210-630 Salvador, BA, Brazil^b Department of Materials Engineering, Federal University of São Carlos, Rodovia Washington Luis, Km 235, 13566-550 São Carlos, SP, Brazil

ARTICLE INFO

Article history:

Received 14 December 2015

Received in revised form 31 March 2016

Accepted 2 April 2016

Available online 13 April 2016

Keywords:

Amorphous alloys

Corrosion resistance

Applications

Crystallization

ABSTRACT

The present article focuses on the current status of research and development concerning corrosion resistance of Fe-Cr-based amorphous alloys and gives suggestions for further investigations aimed at improving the performance of these alloys and recommendations of possible new applications. These materials, which are usually obtained either as glassy bulk material or in coating and ribbon form, show high corrosion resistance and high wear resistance and are also relatively inexpensive compared to other amorphous metallic alloys. These characteristics can lead to promising applications of these alloys in which corrosion resistance and erosion-corrosion resistance are important. This review presents the results obtained in recent years, including the effect of amorphous structure, partial crystallization and composition on corrosion resistance, as well as applications of these alloys. Although advances have been made in studies concerning Fe-Cr-based amorphous alloys, there is an important limitation in terms of using them, which is the issue related to the high Mo content needed to achieve sufficient glass-forming ability and high corrosion resistance, which significantly increases the cost of these alloys. Therefore, the cost/benefit relation of these alloys needs to be improved by studying the effect of composition and structure on corrosion resistance and finding new applications of these alloys. Based on this literature review, possible applications and further investigations of these alloys are suggested.

© 2016 Elsevier B.V. All rights reserved.

Contents

1. Introduction	57
2. Effect of amorphous structure and partial crystallization on the corrosion resistance of Fe-Cr-based amorphous alloys.	57
2.1. Uniformity of the passive film	57
2.2. Higher reactivity of the amorphous structure	57
2.3. Absence of typical defects in the crystalline phase	57
3. Effect of composition on the corrosion resistance of Fe-Cr-based amorphous alloys	59
3.1. Effect of the metalloids B, C and P	59
3.2. Effect of Si	59
3.3. Effect of Mo	60
3.4. Effect of Nb	61
3.5. Effect of Ni	61
4. Applications of Fe-Cr-based amorphous alloys	61
5. Summary and trends for future investigations	63
5.1. Effect of the partial replacement of Mo by Nb	63
5.2. Effect of the partial replacement of Mo and Fe by Si	64
5.3. Effect of the partial replacement of Mo by Ni	64
5.4. Effect of partial crystallization on Fe-Cr-based amorphous alloys containing Si	64
5.5. Use of Fe-Cr-Si-based amorphous alloys as the anode in impressed current cathodic protection systems.	64
References.	64

* Corresponding author.

E-mail address: caldassouza@hotmail.com (C.A.C. Souza).

1. Introduction

Iron-based amorphous alloys have attracted a great deal attention for industrial applications due to the possibility of obtaining alloys with good soft magnetic properties, high corrosion resistance and high wear resistance. In addition, they have a relatively low cost compared to other amorphous metallic alloys, such as those based on Co, Zr, Ni, Cu, Ti, Pd, Co, Ce, Mg, Pt and Au. As occurs in stainless steels, Cr is the most important element for increasing the corrosion resistance of iron-based amorphous alloys [1]. Therefore, their high resistance to corrosion is the main justification for the use of Fe-Cr-based amorphous alloys. In addition to corrosion resistance, these alloys have high wear resistance [2–5], which makes using these alloys promising in applications where the erosion–corrosion resistance is important.

In Fe-Cr-based amorphous alloys, as in stainless steel, a protective hydrated chromium oxyhydroxide film can also be found [6]. Due to its amorphous structure, the protective ability of this passive film base is significantly high, which enables these alloys to have a higher corrosion resistance than that of stainless steel with a similar Cr content.

Fig. 1 [7] shows the mass loss of amorphous and crystalline $\text{Fe}_{67.7}\text{B}_{20}\text{Cr}_{12}\text{Nb}_{0.15}\text{Mo}_{0.15}$ (in at%) alloys in H_2SO_4 solution, indicating that the corrosion resistance of the amorphous alloy is significantly higher than that of the crystalline alloy.

Because of the protective ability of the passive film formed on the amorphous alloy, the minimum amount of Cr in the alloy required to develop the protective film is smaller than that of the crystalline alloy. A critical content of 8.3 at% Cr (9.5 wt%) to form a stable passive film has been proposed from investigations [8] on the corrosive behavior of bulk metallic glasses of $\text{Fe}_{71.4-x}\text{C}_{7.1}\text{Si}_{4.4}\text{B}_{6.5}\text{P}_{8.6}\text{Cr}_x\text{Al}_{2.0}$ at% ($x = 0$, or $x = 2.3$ – 12.3) in 9.7 M H_2SO_4 (50 vol% H_2SO_4) at 343 K. Moreover, in 1 N HCl solutions at 298 K [9], the $\text{Fe}_{67.6}\text{C}_{7.1}\text{Si}_{3.3}\text{B}_{5.5}\text{P}_{8.7}\text{Cr}_{2.3}\text{Mo}_{2.5}\text{Al}_{2.0}\text{Co}_{1.0}$ BMG containing only 2.3 at% Cr showed a corrosion resistance similar to the 304 stainless steel that contains high Cr (19 at% Cr) and Ni (9 at% Ni) contents. This behavior indicates the promising replacement of stainless steel alloys by amorphous alloys in various applications.

Several studies have reported that amorphous Fe-Cr-based alloys have higher corrosion resistance in comparison with commercial alloys with high corrosion resistance, such as 316 stainless steel [10–13] and Ti-6Al-4 V alloys, in corrosive solutions [12,13].

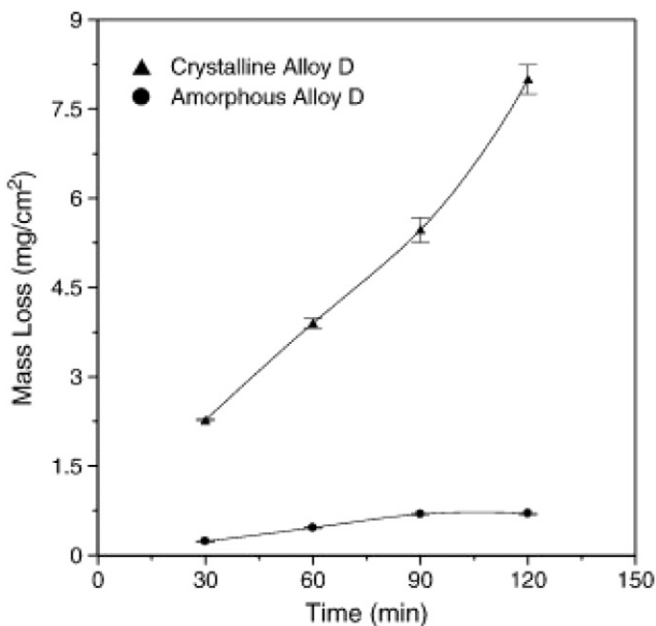


Fig. 1. Mass losses resulting from the immersion of amorphous and crystalline $\text{Fe}_{67.7}\text{B}_{20}\text{Cr}_{12}\text{Nb}_{0.15}\text{Mo}_{0.15}$ alloys in a 0.1 M H_2SO_4 solution [7].

Fe-Cr-based amorphous alloys were primarily obtained as ribbons through a melt-spinning process, whose applications as corrosion resistant material are restricted by the small thickness of these ribbons (usually between 20 and 50 μm in thickness). However, a possible approach to design new compositions for processing millimeter thick rollers or plates, known as bulk metallic glasses (BMG) or bulk amorphous steel (BAS) or to use as coatings is by studying them [14,15].

Using Fe-Cr-based amorphous alloys containing C, B and Mo is promising in various applications [1,10,16,17], which are reported in Section 5, and has resulted in in-depth research carried out in recent years. These alloys generally contain a high content of molybdenum, between 6 and 16 wt%, which significantly increases the cost of these alloys. However, the effect of a large number of alloying elements on the GFA and corrosion resistance of these alloys has been intensively investigated in various corrosive environments. Therefore, this information represents an important tool for the development of Fe-Cr-based amorphous alloys with better cost/benefit ratios for particular corrosive environments. Several review papers [1,16,17] on amorphous alloys have reported information about the magnetic properties, mechanical properties, manufacturing process and corrosion resistance of amorphous Fe-based alloys. Nevertheless, none have focused on the corrosion resistance of amorphous Fe-Cr-based alloys, in spite of the large number of papers reported in the literature focusing on this.

The present review summarizes the details of developments regarding Fe-Cr-based amorphous alloys, including the effect of an amorphous structure, partial crystallization and composition on corrosion resistance and applications of these alloys. The present article also suggests possible applications of these alloys and further investigations aimed at improving their performance.

2. Effect of amorphous structure and partial crystallization on the corrosion resistance of Fe-Cr-based amorphous alloys

The higher corrosion resistance of Fe-Cr-based amorphous alloys in comparison with crystalline alloys of similar composition has been extensively analyzed in the literature and is attributed to the following factors:

2.1. Uniformity of the passive film

Due to the rapid cooling rate, chemical heterogeneities such as precipitates and segregations do not occur in the amorphous structure, resulting in a chemically homogeneous single phase [18,19]. As a result, a more uniform passive film is formed, which is more protective against corrosion. Moreover, a smaller amount of passivating alloying elements, such as Cr, is required in the passive film to achieve the necessary stability [20].

2.2. Higher reactivity of the amorphous structure

The high reactivity of the amorphous structure hastens the formation of a hydrated chromium oxyhydroxide film and increases the concentration of Cr cations in this film, thereby improving its protective capability [18].

2.3. Absence of typical defects in the crystalline phase

Defects, such as dislocations, grain boundaries and second-phase precipitates do not occur in the amorphous structure. These defects can act as galvanic couples and, therefore as sites for the onset of corrosion [18–20].

A recent study [21] using a combination of complementary high-resolution analytical techniques clarified the effect of the structure on the partitioning of elements in an Fe-Cr-Mo-C-B alloy and how this affects the corrosion resistance of the alloy. In this study, although the amorphous alloy had a chemical homogeneity with a uniform elemental

distribution, the fully crystallized alloy showed the presence of Mo-rich and Cr-poor phases. These regions, due to the absence or reduced presence of Cr, act as dissolution sites during the formation of the passive film, resulting in a passive film with greater roughness in comparison with the metal surface prior to passive film formation. Due to a uniform elemental distribution, the roughness of the passive film in the amorphous alloy is significantly lower, which results in a smaller contact area with the corrosive environment and, thus higher resistance to corrosion [21]. However, in this study, the effect of the elemental distribution on the protective ability of the passive film is mainly based on the formation of a Mo-rich phase in the crystalline structure. Therefore, it is interesting to analyze how the protective ability of the passive film is affected by the distribution of elements such as Nb, Ni and Si in the amorphous and crystalline Fe–Cr-based alloys using a combination of complementary high-resolution analytical techniques.

The corrosion resistance of Fe–Cr-based amorphous alloys can be altered by annealing, which causes the structural relaxation of alloys. This phenomenon increases the atomic ordering short distance while maintaining a completely amorphous structure. Table 1 shows the effect of structural relaxation on the corrosion resistance of several Fe–Cr-based amorphous alloys in various corrosive environments. This table indicates that the effect of structural relaxation on the corrosion resistance of Fe–Cr amorphous alloys depends on the alloy composition and corrosive environment.

The improved corrosion resistance of Fe–Cr-based amorphous alloys, due to structural relaxation, is mainly associated with the relief of residual stress, which implies an increase in activation energy, ΔG^* , to redistribute the chemical elements on the surface [24,28] and to decrease the number of active sites for corrosion due to the decrease in quenched-in defects [25]. However, the experimental results show that the effect of structural relaxation on corrosion resistance depends on the alloy composition and the corrosive environment, and this dependency is not clear in the literature.

As observed in Table 1, the effect of structural relaxation on the corrosion resistance of $\text{Fe}_{65.5}\text{Cr}_4\text{Mo}_4\text{Ga}_4\text{E}_{12}\text{C}_5\text{B}_{5.5}$ (in at%) bulk alloy in an HCl solution is beneficial at concentrations of 0.1 and 1 N, but is detrimental at a concentration of 3 N. This effect may be related to the composition of the passive film. The passive film formed after exposure to a 3 N HCl solution contained Cr, Mo and Fe cations [27]; however, the passive film formed after exposure to acetate buffer containing 0.1 N sodium chloride only contained these cations after sub-surface phosphorous enrichment [24]. Structural relaxation and the consequent increase in short order should decrease the activity of this alloy, which would lead to a decrease in the amount of Cr cations found in the passive film, thus damaging its protective capacity. It is likely that this effect predominates in situations in which the structural relaxation reduces the corrosion resistance. However, it is necessary to determine whether the structural relaxation affects the amount of Cr cations in the passive film.

The relative low GFA of Fe–Cr alloys limits the fully amorphous structure thickness to be reached with these alloys. A high Mo content and the addition of alloying elements such as Y and Co are necessary for the formation of a fully amorphous structure, which significantly increases the cost of the alloy. Moreover, to prevent the formation of a

crystalline phase, the BMG alloys are obtained in the form of plates or rods with a thickness of generally less than 1 cm, which restricts the use of these alloys to a limited number of applications. The largest diameter of Fe–Cr-based BMG rods reported is 16 mm, produced with $\text{Fe}_{41}\text{Co}_7\text{Mo}_{14}\text{C}_{15}\text{B}_6\text{Y}_2$ (in wt%) alloy composition [29].

Generally, as already stated, the presence of a crystalline phase in the amorphous structure reduces the corrosion resistance, and this effect is related to the uniformity of the passive film [30]. In addition, the presence of regions with different degrees of susceptibility to corrosion, where the amorphous phase is more corrosion resistant than the crystalline phase, may produce galvanic pairs and increase the dissolution rate in the crystalline regions.

However, it is unclear how the level of partial crystallization of the amorphous alloy affects corrosion resistance. In addition, the effect of partial crystallization on the corrosion resistance of amorphous alloys depends on the alloy composition. In Fe-based “nanocrystalline” ribbons, which are rapidly solidified ribbons presenting a microstructure formed by nanosize crystalline phases embedded in an amorphous matrix, if the Si content is high enough to form passive films, the corrosion resistance increases as the fully amorphous precursor partially crystallizes [31–33]. Examples of nanocrystalline alloys are $\text{Fe}_{78}\text{B}_{13}\text{Si}_9$ and Fe–Cu–Nb–Si–B. The latter is also known as FINEMET. This behavior is attributed to the greater enrichment of Si [34] in the passive layer due to the formation of a large interfacial area between the amorphous and crystalline regions. This area contains numerous defects such as micro voids and free volumes, which favors Si diffusion. Moreover, it is possible that the ultrafine microstructure of nanocrystalline alloys allows for the uniform distribution of impurities and provides a homogenous substrate for the formation of a stable passive layer [30].

The effect of partial crystallization on the structure and corrosion resistance of Fe-based amorphous alloys containing Cr has been investigated in alloys such as $\text{Fe}_{50}\text{Cr}_{15}\text{Mo}_{14}\text{C}_{15}\text{B}_6$ (in at%) ribbons [35], $\text{Fe}_{66.7}\text{C}_{7.0}\text{Si}_{3.3}\text{B}_{5.5}\text{P}_{8.7}\text{Cr}_{2.3}\text{Al}_{2.0}\text{Mo}_{4.5}$ BMG [36], $\text{Fe}_{48}\text{Cr}_{15}\text{Mo}_{14}\text{C}_{15}\text{B}_6\text{Y}_2$ (in at%) BMG [37], and $\text{Fe}_{48}\text{Cr}_{15}\text{Mo}_{14}\text{C}_{15}\text{Y}_2\text{B}_6$ (in at%) coatings [38]. The results obtained show that partial crystallization affects the electrochemical behavior of the amorphous alloy, indicating a decrease in corrosion resistance. However, these partially crystallized alloys showed higher corrosion resistance than the fully crystallized state.

The partial crystallization of Fe–Cr-based amorphous alloys causes the formation of Cr-rich nanocrystalline phases such as $(\text{Fe,Cr})_{23}(\text{C,B})_6$ and $(\text{Fe,Cr})_3\text{B}$ in an $\text{Fe}_{50}\text{Cr}_{15}\text{Mo}_{14}\text{C}_{15}\text{B}_6$ (at%) alloy [35] and $(\text{Fe,Cr})_{23}\text{C}_6$ and $(\text{Fe,Cr})_7\text{C}_3$ in an $\text{Fe}_{48}\text{Cr}_{15}\text{Mo}_{14}\text{C}_{15}\text{B}_6\text{Y}_2$ (at%) alloy [37]. Depending on the composition of the alloy, crystalline phases such as Cr_2B and WC can also form [39]. The presence of these nanosize crystalline phases results in Cr-depleted regions, which leads to a decrease in corrosion resistance [28,37]. In addition to the formation of Cr-rich nanocrystalline phases, partial crystallization of amorphous alloys can also result in the presence of Mo-rich regions in the remaining amorphous phase. The effect of partial crystallization on the corrosion resistance of the $\text{Fe}_{48}\text{Cr}_{15}\text{Mo}_{14}\text{C}_{15}\text{Y}_2\text{B}_6$ (in at%) amorphous coating has been attributed to a decrease in (Cr, Mo)-oxides in the passive film of the coatings due to the preferential formation of (Cr, Mo)-rich carbides, M_{23}C_6 and M_7C_3 ($\text{M} = \text{Fe, Cr, Mo}$) at the intersplat boundaries between the non-melted powders of the coating [38]. Pitting initiated around the Cr-/

Table 1
Effect of structural relaxation on corrosion resistance of Fe–Cr base amorphous alloys in several corrosive environmental.

Alloy composition	Corrosive environmental	Effect on corrosion resistance	Reference
$\text{Fe}_{85}\text{P}_6\text{Cr}_5\text{C}_3\text{Si}$ ribbons	0.5 M H ₂ SO ₄	Increase	[22]
$\text{Fe}_{34}\text{Ni}_{36}\text{Cr}_{10}\text{P}_{14}\text{B}_6$ ribbons	1 N H ₂ SO ₄ and 1 N HCl	Increase	[23]
$\text{Fe}_{65.5}\text{Cr}_4\text{Mo}_4\text{Ga}_4\text{P}_{12}\text{C}_5\text{B}_{5.5}$ (at%) bulk	HCl (0.1 N and 1 N), acetate buffer whit chorides (0.1 N and 1 N), and H ₂ SO ₄ (0.1 N and 1 N)	Increase	[24]
$\text{Fe}_{78-x}\text{Si}_{13}\text{B}_9\text{Cr}_7$ ($x = 3, 4, 5, 7, 9, 10$) (in at%) ribbons	0.5 N KOH	Increase	[25]
$\text{Fe}_4\text{Cr}_5\text{W}_{13}\text{P}_7\text{C}$ ribbon	1 N HCl	Decrease	[26]
$\text{Fe}_{10}\text{Cr}_{13}\text{P}_7\text{C}$ ribbon	1 N HCl	No change	[26]
$\text{Fe}_{65.5}\text{Cr}_4\text{Mo}_4\text{Ga}_4\text{P}_{12}\text{C}_5\text{B}_{5.5}$ (at%) bulk	5% NaCl, 3 N HCl, HNO ₃ , NaOH	Decrease	[27]

Mo-rich carbides at the locations in the amorphous matrix where Cr was depleted [40].

Potentiodynamic polarization curves of Fe₅₀Cr₁₅Mo₁₄C₁₅B₆ (in at%) ribbon alloy revealed that the behavior of the passive film becomes significantly affected only when the partial crystallization is carried out under conditions allowing the formation of the Mo-rich crystalline phase [18,35]. These results indicate that the effect of partial crystallization on the behavior of the passive film, and hence on the corrosion resistance of the alloy, depend on the level of crystallization. Therefore, studies analyzing how increasing the thickness of the partial crystallization of the BMG affects the corrosion resistance are interesting.

The presence of crystalline Fe- α , Fe₂B and FeNbB phases were found in the partially crystalline coating of the Fe₆₀Cr₈Nb₈B₂₄ (at%) alloy [41]. Cr precipitates were not detected in this alloy, which indicates that the content of 8 at% Cr found in the alloy was not sufficient to form these precipitates. Despite the absence of Cr precipitates in the crystalline phase, the partial crystallization significantly decreased the corrosion resistance of the alloy. This behavior is attributed to the formation of the α -Fe and Fe_xB ($x = 1, 2$ or 3) crystalline phases that have greater corrosion susceptibility compared to that of the amorphous phases, promoting internal galvanic effects, and also to the formation of Nb-rich phases, which deplete the matrix of Nb. The increase in corrosion resistance with the partial crystallization reported in a FINEMET alloy (Fe₇₄Cu₁Nb₃Si_{13.5}B_{8.5}) [33] indicates that the effect of increasing the protective capacity of the SiO₂ passive film due to partial crystallization prevailed over the possible formation of the α -Fe and FeB crystalline phases, in addition to the formation of Nb-rich phases.

Therefore, based on the studies reported in the literature [33,41] that show that the effect of the partial crystallization on the corrosion resistance depends on the amorphous alloy composition, it is interesting to analyze the effect of partial crystallization on the corrosion resistance of Fe-Cr-based amorphous alloys containing different amounts of Cr and Si.

Effect of composition on the corrosion resistance of Fe-Cr-based amorphous alloys

Effect of the metalloids B, C and P

3. Effect of composition on the corrosion resistance of Fe-Cr-based amorphous alloys

3.1. Effect of the metalloids B, C and P

Metalloids B, C and P are primarily added to amorphous alloys to promote the amorphous structure, but they also improve the corrosion resistance of the Fe-Cr-based alloy when they partially replace Fe. This enhanced corrosion resistance is related to the effect of these elements on the reactivity of the alloy and on the incorporation of compounds into the passive film [42].

The P, C and B additions in Fe-Cr amorphous alloys accelerate the active dissolution prior to passive film formation and accordingly lead to the increase in beneficial species such as chromium in the passive film, consequently improving the corrosion resistance. In the Fe_(50-x)Cr₁₆Mo₁₆C₁₈B_x ($x = 4, 6$ or 8 at%) BMG [43], increasing the content of B improves the corrosion resistance in the HCl solution. This improvement is attributed to the increase in the chromium concentration in the passive film due to the increase in the B content in the alloy. Nevertheless, the formation of chromium borate also takes place, and due to this there is a decrease in the concentration of chromium oxyhydroxide in the film, which leads to a decrease in the protective quality of the film [42]. The partial substitution of Fe by metalloids is limited by the minimum iron content required to have a high glass forming ability; in Fe_(50-x)Cr₁₆Mo₁₆C₁₈B_x ($x = 4, 6, 8$ or 10 at%) BMG, this limit corresponds to 40 at% Fe.

The addition of P is more effective to improve corrosion resistance than B [42]. This effect is due to the high reactivity of this element, which accelerates the active dissolution of alloys prior to the passive

film formation, allowing for the rapid formation of a passive film. C also promotes the active dissolution of alloys, but this effect is less significant compared to P [42]. However, in spite of several studies reported in the literature, it is not clear how the presence of metalloids accelerates the active dissolution of amorphous alloys.

A study of the active dissolution of BMG (Fe_{44.3}Cr₅Co₅Mo_{12.8}Mn_{11.2}C_{15.8}B_{5.9})_{98.5}Y_{1.5} (at%) revealed that the presence of C accelerates the active dissolution of alloys due to the formation of gaseous products such as CO₂ and CH₄ on the surface of the alloy [44]. According to this study, these gases form bubbles that burst and cause the localized breakdown of the oxide film and the C layer, which leads to a more active reaction in comparison with the absence of C in the alloy.

Although metalloids B, P and C additions affect the corrosion resistance, the presence of these elements in the Fe-Cr-based amorphous alloys is mainly determined by their effect on the GFA of the alloy. Several bulk metallic glasses with high GFA and corrosion resistance contain C and B, with C at a higher concentration. In the Fe₄₃Cr₁₆Mo₁₆(C,B,P)₂₅ (wt%) BMG system [45], the Fe₄₃Cr₁₆Mo₁₆C₁₅B₁₀ (wt%) alloy corresponds to the composition with higher GFA, allowing a BMG with a 2.7 mm diameter to be obtained. Moreover, the partial substitution of B by C and P resulted in the Fe₄₃Cr₁₆Mo₁₆C₁₅B₅P₅ (wt%) alloy with increased corrosion resistance in HCl solution, although at a loss to reduce the GFA allowing the production of BMG with a maximum diameter of 2.2 mm.

3.2. Effect of Si

Si addition in Fe-Cr based amorphous alloys to improve GFA has been reported in coatings, such as Fe_{49.7}Cr₁₈Mn_{1.9}Mo_{7.4}W_{1.6}B_{15.2}C_{3.8}Si_{2.4} (in wt%) [46] and Fe₇₀Cr₁₅Mo₄P₅B₄C₁Si₁ (in wt%) [47], in ribbons such as Fe₆₂Cr₁₀Ni₈Si₂₀ [48] and Fe₄₇Co₇Cr₁₅Mo_{4.5}Nb_{4.5}Si₅B₁₅Y₂ (in at%) [49], as well in bulk such as Fe_{57.6}C_{7.1}Si_{3.3}B_{5.5}P_{8.7}Cr_{12.3}Mo_{2.5}Al_{2.0}Co_{1.0} (in wt%) [50] and Fe_{59.1}C_{7.1}Si_{4.4}B_{6.5}P_{8.6}Cr_{12.3}Al_{2.0} [8]. Particularly in soft-magnetic bulk amorphous alloys, Si addition has been reported for Fe_{66.7}C_{7.0}Si_{3.3}B_{5.5}P_{8.7}Cr_{2.3}Al_{2.0}Mo_{4.5} (in wt%) [51] and Fe_{41.5}Co_{27.6}B_{18.4}Si_{5.5}Nb_{3.8}Cr₄ alloys [52].

Besides its influence on GFA, Si additions can increase the corrosion resistance. This effect is very well known in soft magnetic alloys, such as Fe-C-Si-B-P-Cr-Al amorphous alloys [8] and Fe-Cu-Nb-Si-B nanocrystalline alloys [24], and is related to the formation of SiO₂ passive films [8]. In the Fe_{59.1}C_{7.1}Si_{4.4}B_{6.5}P_{8.6}Cr_{12.3}Al_{2.0} (in at%) alloy [8], the Si content is high enough to form a SiO₂ passive film that promotes corrosion resistance. The formation of this film occurs from the diffusion of Si to the surface of the alloy:



As observed in reaction (1), the formation of the SiO₂ passive film depends on diffusion of Si up to the alloy surface. Therefore, factors that favor this diffusion process, such as the partial crystallization of the amorphous structure analyzed in Section 2 and the presence of Ni in the alloy composition can favor SiO₂ passive film formation, thus increasing the protective capacity of the film.

High corrosion resistance of Fe-Ni-Si-B amorphous ribbons is a good example [53] where Ni promotes α -Fe nucleation, resulting in a larger area of the interfaces between the nuclei and matrix regions. This interface, similar to the interfaces between the nanocrystalline and matrix regions of partially crystallized alloys, may contain numerous defects such as microvoids and free volumes, which favors Si diffusion. Therefore, further studies to analyze the effect of Si addition on the corrosion resistance of Fe-Cr-based amorphous alloys containing Ni are interesting.

Besides the formation of the SiO₂ passive films, Si addition in Fe-Cr-based amorphous alloys may also affect the composition and uniformity of chromium oxide passive films, making this film more protective. For

$\text{Fe}_{62}\text{Cr}_{10}\text{Ni}_8\text{X}_{20}$ ($\text{X}=\text{P}, \text{B}, \text{Si}$) amorphous alloy ribbons submitted to 0.01 M HCl solution, Si addition leads to higher corrosion resistance when compared with P addition, and this behavior is explained by the presence of Ni and Fe oxides, as well as Cr oxide observed in the P content alloy [54].

It is important to consider that the addition of Si to Fe–Cr-based amorphous alloys, as well as the improvement in GFA and corrosion resistance, due to the low cost of Si, makes the partial substitution of high-cost elements such as Mo, Nb and Ni by Si promising.

Fig. 2 shows the potentiodynamic polarization curves of $\text{Fe}_{47}\text{Co}_7\text{Cr}_{15}\text{Nb}_7\text{Mo}_7\text{B}_{15}\text{Y}_2$, $\text{Fe}_{41}\text{Co}_7\text{Cr}_{15}\text{Mo}_{14}\text{C}_{15}\text{B}_6\text{Y}_2$ and $\text{Fe}_{47}\text{Co}_7\text{Cr}_{15}\text{Nb}_{4.5}\text{Mb}_{4.5}\text{Si}_{15}\text{B}_{15}\text{Y}_2$ amorphous ribbons (in at%) in comparison with 316 stainless steel. The polarization curves were carried out at a scan rate of 2 mV s^{-1} in a 4.0 M solution of HCl, using the alloy ribbons as the working electrode. These curves were obtained from a potentiostatic/galvanostat EG&G 273. The auxiliary electrode was a graphite cylinder, and a saturated calomel electrode (SCE) was used as a reference. These curves present a region in which the current density has a small variation in its potential, showing that the passive film was formed. A smaller value of the current density in the passive region, *ip*, for the amorphous ribbons is related to a more protective passive film. These results indicate that the partial replacement of Mo and Nb by Si in amorphous alloys reduces the protective capability of the passive film. However, this capability is still better than the 316 stainless steel. Therefore, it is interesting to establish the maximum amount of Mo and Nb that can be replaced by Si while maintaining an amorphous alloy with higher corrosion resistance to 316 stainless steel.

3.3. Effect of Mo

In general, the Fe–Cr-based amorphous alloys with high corrosion resistance reported in the literature contain a high content of Mo, from 6 at% to 16 at%. These alloys are obtained as BMG, ribbons or coatings and show high resistance to corrosion in a concentrated HCl solution with measured corrosion rates of 1–10 $\mu\text{m}/\text{year}$ [1]. In Table 2, typical Fe–Cr-based alloys containing Mo with higher corrosion resistance are reported.

As observed previously, the high corrosion resistance of Fe–Cr based amorphous alloys is mainly attributed to the formation of a Cr-enriched oxy hydroxide passive film. XPS analysis revealed the presence of Mo cations (Mo^{+4} , Mo^{+5} and Mo^{+6} states) in passive films formed on Fe–Cr–Mo–C–B metallic glasses exposed to air and also during immersion in 1 N HCl solution [43]. The presence of Cr^{3+} was detected in this passive film in a larger amount than the Mo ions, indicating that Cr has the most significant effect on the protective ability of the passive film in comparison with Mo.

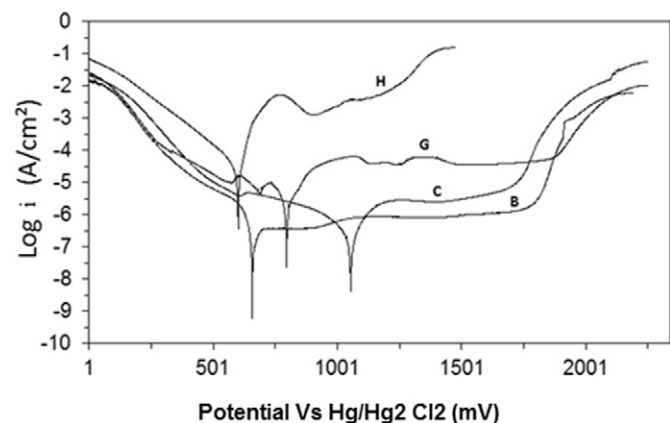


Fig. 2. Potentiodynamic polarization curves obtained in a 4.0 M solution of HCl at a scan rate of 2 mV/s of alloys B ($\text{Fe}_{47}\text{Co}_7\text{Cr}_{15}\text{Nb}_7\text{Mo}_7\text{B}_{15}\text{Y}_2$), C ($\text{Fe}_{41}\text{Co}_7\text{Cr}_{15}\text{Mo}_{14}\text{C}_{15}\text{B}_6\text{Y}_2$), G ($\text{Fe}_{47}\text{Co}_7\text{Cr}_{15}\text{Nb}_{4.5}\text{Mb}_{4.5}\text{Si}_{15}\text{B}_{15}\text{Y}_2$) and H (stainless steel 316).

Although the effect of Mo addition to enhance resistance to general corrosion and pitting corrosion in amorphous alloys is well known, the mechanism of how this effect takes place is still unclear. It is stated that this effect is mainly related to the synergistic effects of Cr and Mo.

The addition of Mo in the alloy can promote the enrichment of Cr in the passive film and consequently enhances the corrosion resistance of the alloy [60,61]. However, this effect depends of polarization and solution conditions. It has been reported [60] that when the potential of amorphous Fe–Cr–Mo–P–C alloy is lies in the passive potential region of chromium and molybdenum and immersed in aerated solution the addition of Mo in the alloy promotes the enrichment of Cr in the passive film. However when these conditions are not complied the addition of molybdenum no promotes the enrichment of Cr in the passive film of alloy.

The presence of Mo cations was also observed by Gostinet al. [62] in the corrosion products layer of bulk glassy ($\text{Fe}_{44.3}\text{Cr}_5\text{Co}_5\text{Mo}_{12.8}\text{Mn}_{11.2}\text{C}_{15.8}\text{B}_{5.9}$) $_{98.5}\text{Y}_{1.5}$ (at%) alloy after immersion in 0.5 M H_2SO_4 and 1 M HCl. According to the authors, this element appeared to be in an oxidized state, corresponding to MoO_3 and MoO_2 . The presence of Mo cations in the passive film indicates the possibility of the formation of a Mo oxide passive film on the alloy surface. The formation of a Mo-enriched passive film is possible in Fe-based amorphous alloys when the enrichment of Cr ions in the surface film becomes insignificant. When the contents of Cr and Mo in the amorphous alloy are polarized at the potential in the passive region of Mo and the active region of Cr, the corrosion resistance of the alloy in de-aerated HCl solution is related to the formation of passive tetravalent Mo oxyhydroxide [63]. However, the passive film of Mo shows lower stability in comparison with the passive hydrated chromium or iron oxyhydroxide film [1,63], and thus the joint presence of Mo and Cr passive films is not possible.

It is likely that the presence of Mo in amorphous alloy may also result in the formation of a more compact passive film with Mo ions occupying the empty spaces in the passive film, making the passive film more compact and therefore more protective. However, it is necessary to experimentally verify this effect.

The effect of Mo on the corrosion behavior of amorphous Fe–Cr-based alloys depends on the pH of the corrosive medium. In acidic solution, the ($\text{Fe}_{44.3}\text{Cr}_5\text{Co}_5\text{Mo}_{12.8}\text{Mn}_{11.2}\text{C}_{15.8}\text{B}_{5.9}$) $_{98.5}\text{Y}_{1.5}$ (at%) BMG amorphous alloy shows a much higher stability (lower critical current densities and nobler passivation potentials) than the conventional stainless steel X210Cr12 [62]. However, in very alkaline solution, 1 M NaOH (pH 14), the amorphous alloy has a lower stability than the conventional steel. This behavior is attributed to the dissolution of Mo, Co and Mn in very basic solutions.

The effect of Mo on the increase in GFA may be related to the empirical component rules for achieving high GFA [64]. The addition of Mo enables the generation of new atomic pairs with large negative heats of mixing, such as Mo–Fe, Mo–B and Mo–P, that lead to a highly stable supercooled liquid and, therefore to the inhibition of the nucleation kinetics of the crystalline phase [65]. In general, Mo and Nb have the largest atomic sizes in the Fe-based alloy system, which favors the greater difference in atomic size ratios among the main constituent elements. This greater difference in atomic size ratios leads to more efficient packing, thus favoring the liquid's stability. A larger number of alloying elements could lead to an increase in the GFA because the tendency to form all-crystalline phases can be difficult. Thus, from this point of view, the addition of Mo could also improve the GFA.

In some Fe–Cr-based amorphous alloys containing Mo, alloying elements such as W, Y, Mn and N are also added. In these cases, the presence of Y increases the GFA while W increases the pitting corrosion resistance [66,67]. In Fe–Cr-based amorphous alloys, Mn is added in high amounts to alloys such as ($\text{Fe}_{44.3}\text{Cr}_5\text{Co}_5\text{Mo}_{12.8}\text{Mn}_{11.2}\text{C}_{15.8}\text{B}_{5.9}$) $_{98.5}\text{Y}_{1.5}$ (at%) in which the combination of high GFA and excellent mechanical performance are more important than the corrosion resistance. However, in amorphous alloys that have high corrosion resistance, such as $\text{Fe}_{49.7}\text{Cr}_{17.7}\text{Mn}_{1.9}\text{Mo}_{7.4}\text{W}_{1.6}\text{B}_{15.2}\text{C}_{3.8}\text{Si}_{2.4}$, Mn is added in low amounts [68].

Table 2

Typical Fe–Cr-based alloys containing Mo with higher corrosion resistance are reported together with their synthetic method, BMG thickness (t_{\max} /mm), and environment in which the corrosion resistance was evaluated.

Alloy composition	Synthetic method	t_{\max} /mm	Environment	Reference
Fe ₄₉ Cr _{15.3} Mo ₁₅ Y ₂ C ₁₅ B _{3.4} N _{0.3} (at%)	Cu mold casting	1.2	6 M HCl	[55]
Fe ₄₃ Cr ₁₆ Mo ₁₆ C ₁₀ B ₅ P ₁₀	Cu mold casting	2.7	6 M HCl	[45]
Fe _{54.2} Cr _{18.3} Mo _{13.7} Mn ₂ W ₆ B _{3.3} C _{1.1} Si _{1.4} (wt%)	HVOF sprayed	–	3.5 wt% NaCl	[56]
Fe ₄₃ Cr ₁₆ Mo ₁₆ C ₁₅ B ₁₀ (at%)	HVOF sprayed	–	3.5 wt% NaCl and 0.5 M H ₂ SO ₄	[57]
Fe _x Cr _{10.9} Mo _y P _{13.1} C _{8.36} Si _{0.77} (at%)	HVOF sprayed	–	1 N H ₂ SO ₄ and 1 N HCl	[58]
Fe ₄₈ Cr ₁₅ Mo ₁₄ C ₁₅ B ₅ Y ₂	HVOF sprayed	–	1 M HCl	[59]
Fe ₄₂ Cr ₁₆ Mo ₁₆ C ₁₈ B ₈ (at%)	Cu mold casting	1.2	6 N HCl	[43]

N addition, as in the Fe₄₉Cr_{15.3}Mo₁₅Y₂C₁₅B_{3.4}N_{0.3} (at%) BMG alloy, increases corrosion resistance concerning the concentrated HCl environment [69]. This behavior is attributed to the enrichment of Cr oxide and the presence of MoN nitrides on the surface of the passive layer. These nitrides, which are negatively charged, such as MoN[−], repel the aggressive Cl[−] ions.

3.4. Effect of Nb

Nb is the transition metal that is commonly used in Fe-based soft magnetic alloys, such as NANOPERM and FINAMET, both nanocrystalline alloys. In these alloys, Nb inhibits grain growth and with the presence of Cr, Nb is mainly used in soft-magnetic bulk amorphous alloys, such as Fe–Co–B–Si–Nb–Cr [70,71] at a concentration of approximately 4 wt% and Fe–P–B–Nb–Cr [72] at a concentration of 1 wt%. To increase the corrosion resistance of these alloys without harming their magnetic properties, Cr is added in small amounts, between 1 and 4 at% [70–72].

There are very few Fe–Cr-based amorphous alloys containing Nb reported in the literature. An investigation of Fe₅₅ – xCr₁₈Mo₇B₁₆C₄Nb_x (x = 0, 3 or 4 at%) amorphous ribbons in Ringer's solution revealed that the corrosion resistance significantly increases with an increase in the Nb content [73]. The addition of small amounts of Nb (0.3 wt%) was enough to increase the uniform corrosion resistance and the pitting corrosion resistance; particularly the Fe₅₁Cr₁₈Mo₇B₁₆C₄Nb₄ (at%) shows higher corrosion resistance compared with 316 L stainless steel and Ti–6Al–4V. The corrosion resistance of Fe₆₀Cr₈Nb₈B₂₄ (in at%) ribbon was evaluated in chloride-rich media at different pH values (3.0, 5.5 and 10.0), and the pH of the environment, unlike alloys containing Mo, did not affect the corrosion resistance of the alloy [74].

In alloys containing Mo, the partial substitution of Mo by Nb can increase the corrosion resistance of the amorphous alloy; In Fe₄₅Cr₁₆Mo₁₆C₁₈B₅ and Fe₄₅Cr₁₆Mo₁₄Nb₂C₁₈B₅ glassy ribbon, the last composition presents a higher corrosion resistance in HCl solutions [75].

The increase in corrosion resistance due to partial substitution of Nb for Mo was also observed in amorphous alloys containing small amounts of Nb and/or Mo (0.3 wt%) [7]. In ribbons of Fe₆₈B₂₀Cr₁₂, Fe_{67.7}B₂₀Cr₁₂Mo_{0.3}, Fe_{67.7}B₂₀Cr₁₂Nb_{0.3} and Fe_{67.7}B₂₀Cr₁₂Nb_{0.15}Mo_{0.15} (in at%) alloys, the alloy containing both Nb and Mo presented higher corrosion resistance than alloys containing just one of these elements, in H₂SO₄ and NaCl solution.

The effect of Nb in enhancing corrosion resistance can be attributed to the presence of Nb₂O₅ in the passive film, which increases the susceptibility to passivation and the protective capacity of passive film. The presence of this oxide was detected by XPS analysis of the passive film in FeNbZrCuB amorphous alloy [76]. However, it is unclear whether there would be a synergetic effect between Mo and Nb. To understand this effect, using a combination of complementary high-resolution analytical techniques, such as an inductively coupled plasma mass spectrometer (ICP-MS) and an atom tomography probe (ATP), is suggested.

Concerning the GFA of Fe–Cr-based amorphous alloys, it can be enhanced by substituting a certain amount of Fe or Mo by Nb. The presence of 4 at% Nb in the Fe₄₆Cr₁₅Mo₁₄C₁₅B₆Nb₄ alloy increases the

diameter of a fully amorphous structured sample from less than 1 mm (without Nb) to 3 mm. [70]. This effect has also been observed in Fe₄₇Co₇Cr₁₅Mn₉Si₅B₁₅Y₂ (M = Mo, Nb) (in wt%) ribbon alloys [56]. Research on Fe₅₀ – xCr₁₅Mo₁₄C₁₅B₆Nb_x (x = 0, 2, 4 or 6 at%) BMG alloys revealed that there is an optimum content of Nb of 4 at%, above which the GFA of the alloy decreases, which may be related to the formation of a Fe₂Nb crystalline phase [77].

In the same way as Mo, the effect of Nb on the increase in GFA may be related to the empirical component rules for achieving high GFA [7]. The addition of Nb enables the generation of new atomic pairs with large negative heats of mixing such as Nb–Fe, Nb–B and Nb–P, and Nb has a large atomic size, which favors a greater difference in the atomic size ratios among the main constituent elements. The increase in GFA due to the addition of Nb can also be related to the formation of Nb oxides. During the melting and casting processes, it is likely that oxygen in the molten liquid is partially neutralized into Nb oxides, thus stabilizing the remaining liquid [77].

3.5. Effect of Ni

The presence of Ni in Fe-based amorphous alloys improves the corrosion resistance and GFA of the alloy. Ni is the element in the iron group metals with the highest corrosion resistance, and it is well known that the effect of Ni on corrosion resistance is due to the formation of highly protective NiO₂ oxides. The partial replacement of Fe by Ni enhanced the corrosion resistance of [(Fe₁ – xNi_x)_{0.75}B_{0.2}Si_{0.05}]₉₆Nb₄ (x = 0, 0.2 or 0.4) BMG in NaCl, NaOH and H₂SO₄ solutions, and this improvement was most significant in the [(Fe_{0.6}Ni_{0.4})_{0.75}B_{0.2}Si_{0.05}]₉₆Nb₄ BMG [78]. This effect is attributed to the higher protective capacity of NiO₂ compared with the porous iron oxide film.

Investigation of Fe₅₆Cr₂₃Ni_{5.7}B₁₆, Fe₅₃Cr₂₂Ni_{5.4}B₂₃ and Fe₅₀Cr₂₂Ni_{5.6}B₁₉ (in at%) ribbon alloys reported higher corrosion resistance than the alloy SS 316 LN [79].

The effect of the addition of Ni on the corrosion resistance of amorphous alloys has also been compared with the effects of Nb and Cu by evaluating the electrochemical behavior of Fe₅₅M₂Cr₁₂Mo₁₀B₆C₁₃Y₂ (M = Ni, Cu, Nb) [80] (in at%) BMG; the alloy containing Ni showed the best corrosion resistance compared with alloys containing Cu and Nb in NaCl and HCl solutions.

Concerning GFA, the addition of 5 at% Ni to replace Fe in the Fe₇₀Mo₅P₁₀C₁₀B₅ alloy increased the supercooled liquid region ($\Delta T_x = T_x - T_g$; T_x: crystallization temperature; T_g: glass transition temperature), indicating enhanced GFA [81].

4. Applications of Fe–Cr-based amorphous alloys

In recent years, there has been increasing interest in the application of Fe–Cr-based amorphous alloys. As described in Section 1, these alloys can be obtained mainly in the form of ribbons obtained by melt spinning, coatings, and bulk metallic glasses (BMG). The range of compositions that can be processed as BMG and coatings is more restricted than the range that can be produced as ribbons and powders due to differences in the achievable cooling rates [1]. However, the use of these alloys in ribbon form is restricted due to the small thickness of the ribbon.

As detailed in Section 2, the Fe–Cr-based BMG or BAS alloys are obtained in the form of cylinders or plates, with reports of obtaining completely amorphous cylinders with thicknesses up to 16 mm. The high fracture strength, high wear resistance, excellent corrosion resistance, and high thermal stability of Fe–Cr-based BMG [1,81–88] make these materials promising for several applications. Furthermore, the possibility of obtaining the Fe–Cr-based BAS using commercial grade raw materials instead of pure elements has been reported, which reduces manufacturing costs [89]. The higher corrosion resistance of the $\text{Fe}_{51}\text{Cr}_{18}\text{Mo}_{7}\text{B}_{16}\text{C}_{4}\text{Nb}_{4}$ (at%) amorphous alloy compared with 316 L stainless steel and Ti–6Al–4V in Ringer's solution, which is similar to the corrosive environment present in the human body, and the good biocompatibility of this amorphous alloy makes this alloy promising to use in biomedical implants [73].

One of the most promising applications of Fe–Cr-based BMG is as cutting instruments in applications where corrosion resistance is important but impact resistance is not required, such as in surgical tools. The $\text{Fe}_{41}\text{Cr}_{15}\text{Co}_{7}\text{Mo}_{14}\text{C}_{12}\text{B}_{9}\text{Y}_{2}$ BMG blade has much better sharpness than the commercial stainless steel blades, presenting better durability in cutting, testing and higher corrosion resistance [74].

However, Fe–Cr-based BMG alloys have a very low plastic strain at room temperature, which restricts the use of these alloys to applications in which a significant toughness is not required. The presence of Cu in $(\text{Fe}_{0.432}\text{Co}_{0.288}\text{B}_{0.192}\text{Si}_{0.048}\text{Nb}_{0.04})_{0.99}\text{Cr}_{0.01}\text{Cu}_{0.3}$ BMG results in a plastic strain of more than 2.2% before fracturing [82]. However, the addition of Cu promotes the formation of the α -Fe nanocrystalline phase that can damage the corrosion resistance of the alloy [90].

Several studies have found that the Fe–Cr-based amorphous coatings have higher corrosion resistance, and in environments containing chloride, this corrosion resistance is significantly higher than that of austenitic stainless steel alloys, such as 316 stainless steel [39,59,91]. In addition to high corrosion resistance, it has also been reported that these coatings show high wear resistance [5,92]. These characteristics make the use of amorphous Fe–Cr based coatings promising in applications where the resistance to erosion-corrosion (E–C) failure is important. In these applications, material deterioration is caused by the combined action of corrosion and mechanical wear.

In a study involving several coatings obtained from a high-velocity oxyfuel (HVOF) process, $\text{Fe}_{49.7}\text{Cr}_{17.7}\text{Mn}_{1.9}\text{Mo}_{7.4}\text{W}_{1.6}\text{B}_{15.2}\text{C}_{3.8}\text{Si}_{2.4}$ and $\text{Fe}_{48}\text{Mo}_{14}\text{Cr}_{15}\text{Y}_{2}\text{C}_{15}\text{B}_6$ presented a better behavior [39]. Bending tests verified that the glassy-alloy-coated layer in a Fe–Cr–Mo–C–B system showed good cohesion on a 304 stainless steel substrate and a wear resistance greater than the hard chromium plating plate [5,92]. However, the coating performance significantly depends on the feedstock powder size and thermal spraying conditions [17].

The literature contains several suggested applications of Fe–Cr-based amorphous coatings to protect metallic substrates against corrosive and abrasive wear. These applications include the use of these coatings on waste packages, on ship decks and on disk cutters for tunnel-boring machines [93]. In addition, these coatings are considered promising to use on marine pump impellers [94] and containers used to store SNF (spent nuclear fuel) [39]. In relation to this application, a $\text{Fe}_{49.7}\text{Cr}_{17.7}\text{Mn}_{1.9}\text{Mo}_{7.4}\text{W}_{1.6}\text{B}_{15.2}\text{C}_{3.8}\text{Si}_{2.4}$ coating was shown to present exceptional neutron absorption cross-sections [39].

The $\text{Fe}_{54.2}\text{Cr}_{18.3}\text{M}_{18.7}\text{Mn}_2\text{W}_6\text{B}_{13}\text{C}_{1.1}\text{Si}_{1.4}$ (in wt%) amorphous coating on marine pump impellers presented an E–C rate ($\text{mg}/\text{cm}^2 \cdot \text{h}$) that was significantly less than that of 304 stainless steel alloy at several flow rates [94]. Moreover, the FeNiCrBSiNbW coating, which consists of an amorphous phase and a α -(Fe, Cr) nanocrystalline phase, showed higher cavitation erosion resistance compared with the 316 L coating due to the amorphous/nanocrystalline structure of the former material [95]. The high corrosion resistance against cavitation erosion is very important in equipment such as pumps, hydraulic turbines and ship propellers. Therefore, the performance of Fe–Cr-based amorphous coatings reported in the literature also makes their use promising in these applications. Propeller ships generally utilize nickel aluminum

bronze, and the replacement of this alloy by 304 stainless steel coated with the amorphous coating could reduce the cost of the propeller. Austenitic stainless steel is most resistant to cavitation compared with nickel aluminum bronze [96]. However, it is necessary to evaluate whether the presence of nanocrystalline phase does not compromise the pitting corrosion resistance of the coating.

The high erosion-corrosion resistance of Fe–Cr-based amorphous coatings makes the use of these coatings promising in applications that generally use WC-based thermal sprayed coatings [97]. HVOF WC-based sprayed coatings containing Co and Cr have high resistance to corrosion and erosion [98]. However, due to the high cost of these coatings, Fe–Cr-based amorphous coating may have a better cost/benefit ratio in several applications. Examples of applications for which it is interesting to evaluate the performance of amorphous Fe–Cr-based coating include the vanes of sulfation equipment and in mirror heat exchangers in contact with abrasive flow.

In sulfation equipment, homogenization of the mixture consisting of a ground ore and concentrated sulfuric acid (sulfate process) occurs through the movement of vanes fixed on a shaft. One application of this equipment is the production of TiO_2 pigments used in paints. Fig. 3 shows a schematic representation of this equipment.

In aggressive environments, such as environments containing chloride and sulfate, concrete coating is not enough to protect the reinforcing bars from corrosion. Therefore, in these environments, taking additional measures to protect the reinforcing bars against corrosion is recommended. One such measure is using stainless steel reinforcing bars in concrete structures such as austenitic stainless steel 304 and alloy 316 and duplex stainless steel 2205 alloy. These alloys are mainly applied in splash zones, external reinforcements of bridges and foundations, steps and reinforcement joints and connections between prefabricated parts. Based on the reduction of maintenance costs and repair, and the increase in the life of the structure, it has been estimated that the use of stainless steel reinforcements is economically viable when the increase in the initial cost of construction in splash zone regions does not exceed 14% [99]. An alternative to reduce the cost of stainless steel reinforcements could be the use of carbon steel coated with an Fe–Cr-based amorphous alloy because this coating has a cost/benefit rate greater than that of stainless steel alloys.

Investigations into the use of Fe-based amorphous coatings in the steel reinforcing bars of reinforced concrete structure should be carried out in similar conditions to those found in the concrete, which has a pH of approximately 12. In general, tests to evaluate the corrosion resistance of the steel reinforcing bars in reinforced concrete structures are performed in saturated $\text{Ca}(\text{OH})_2$ containing various concentrations of chloride.

As mentioned previously, when Mo is present in Fe–Cr-based amorphous alloys, the alloys tend to dissolve in alkaline media, causing a significant decrease in the corrosion resistance of the alloy. However, in relation to Fe–Cr-based amorphous alloys containing Ni ($\text{Fe}_{56}\text{Cr}_{23}\text{Ni}_{5.7}\text{B}_{16}$, $\text{Fe}_{53}\text{Cr}_{22}\text{Ni}_{5.4}\text{B}_{23}$ and $\text{Fe}_{50}\text{Cr}_{22}\text{Ni}_{5.6}\text{B}_{19}$), the corrosion resistance of these alloys in solutions of different pH (neutral solution with $\text{pH} = 7.0$ and alkaline solution with $\text{pH} = 10.0$) was

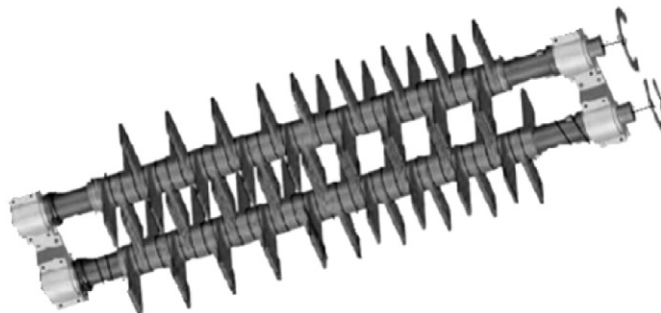


Fig. 3. Schematic representation of sulfation equipment.

verified to be independent of the pH of the corrosive medium [79]. Therefore, these results indicate that the development of amorphous alloys that can show high resistance to corrosion in the presence of chloride in an alkaline medium, with a pH of approximately 12, is necessary.

Moreover, the possibility of using Fe-based amorphous alloys containing Cr as the anode in impressed current cathodic protection systems should be analyzed. Ti anodes coated with noble metals (Ti/MMO) and Fe-Si-Cr anodes are usually used in protection systems in environments containing chloride. The Fe-14.5%Si-4.5%Cr crystalline alloy is a typical alloy used as the anode in impressed current cathodic protection systems. The Fe-Si-Cr anode costs significantly less than the Ti-based anode, but the Ti-based alloy generally has a better cost/benefit ratio in environments containing chloride due to the higher corrosion resistance of this alloy [100]. In addition to a low consumption rate, it is important that the anode shows a high density of a permissible current, which is related to the ability of the electrode to withstand high currents.

The performance of the metal anode is related not only to the protective ability of the passive film, but also the resistivity of the film. The function of the anode is to conduct the DC protective current into the environment [101]. Therefore, the presence of a less voluminous passive film implies in lower resistance film to current conduction and, consequently a higher efficiency of the anode [102].

The Fe-based amorphous alloy containing Cr, as previously seen, has a passive film more resistant to dissolution in comparison with the passive film found in the crystalline alloy of the same composition. Moreover, it has been observed [18] from potentiodynamic polarization curves that the Fe-based amorphous alloys have a lower active/passive transition current density in comparison with the crystalline alloys which indicates the presence of a less voluminous passive film. However, as well as the characteristics of the passive film, the performance of the anode depends on the ability to carry out an alternative anode reaction. Therefore, it is interesting to analyze the performance of the amorphous alloy such as Fe-Si-Cr-based alloy as an anode in impressed current cathodic protection systems.

An application in which it would be interesting to analyze the performance of the anode constituted by the Fe-Cr-Si-based amorphous alloy is in the impressed current cathodic protection system of the steel reinforcing bars in reinforced concrete structures. In this system, the anode can be used in ribbon form (width between 10 and 20 mm), which favors obtaining the alloy with a completely amorphous

structure. Therefore, it is interesting to study the performance of anodes composed of Fe-Cr-Si-based amorphous ribbons in this application. This protection system involves the permanent application of a continuous electrical current between the steel reinforcing bars and an external anode, usually the ribbon of the Ti-based material (Ti/MMO) [103]. Fig. 4 shows a schematic representation of the application of impressed current cathodic protection in a reinforced concrete structure.

5. Summary and trends for future investigations

Fe-Cr-based amorphous alloys have attracted increasing interest mainly due to their high resistance to corrosion and also to other properties such as wear resistance, a reduction of maintenance costs and exceptional neutron absorption cross-sections. These alloys have been mainly studied in the form of ribbons, bulks and coatings, and the use of these alloys as a protective coating for metallic substrates is their most promising application. However, according to the literature, the alloys that perform better have a high Mo content (between 6 and 16%), which significantly increases their cost. Moreover, the Mo contained in the amorphous alloy can dissolve in an alkaline medium, resulting in lower corrosion resistance.

Studies of Fe-Cr-based amorphous alloys have provided extensive information on the effect of their structure and composition on their behavior, which provides important information to improve the cost-benefit relationship and to propose new applications for these alloys. This review summarizes these results, and the following are suggested further investigations of these alloys and justifications for these suggestions based on information obtained from the literature.

5.1. Effect of the partial replacement of Mo by Nb

As discussed in Section 3.4, Nb and Mo addition to Fe-Cr based alloys has a synergistic effect, and is responsible for the better performance in corrosion resistance and GFA compared with alloys containing each element alone. Considering, as reported in Section 3.4, that the partial replacement of Fe by Nb in an FeCrMoCB amorphous alloy increases the GFA of the alloy significantly, studies on the partial replacement of Mo by Nb in this alloy system to determine the optimum levels of Nb and Mo in relation to the corrosion resistance and GFA of the alloy would be very interesting. Considering that Mo dissolves in alkaline environments, the evaluation of these alloys in environments containing

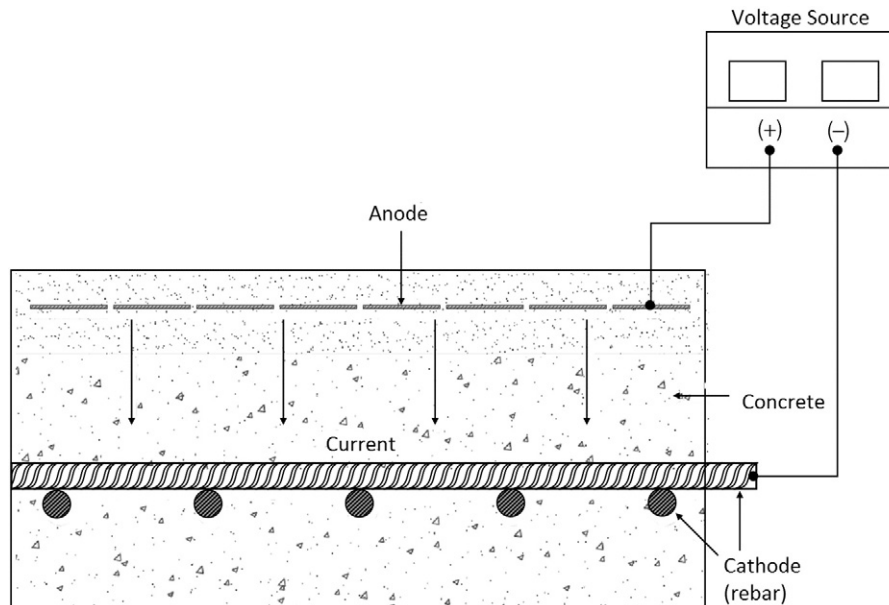


Fig. 4. Schematic representation of the application of impressed current cathodic protection in a reinforced concrete structure [101].

different chloride concentrations and pH values (acid, neutral and basic) would be interesting, including a saturated solution of $\text{Ca}(\text{OH})_2$ at pH 12 containing chloride.

5.2. Effect of the partial replacement of Mo and Fe by Si

As observed in Section 3.2, the addition of Si to Fe–Cr-based amorphous alloys can promote corrosion resistance of this alloy due to the formation of a passive film of SiO_2 . Therefore, considering the relatively low cost of Si, studies should analyze the effect of the partial replacement of Mo and Fe by Si on the corrosion resistance and GFA of the alloy, for instance the Fe–Cr–Mo–Y–C–B alloy. As presented in Section 3.3, the partial substitution of Mo by Si decreases the corrosion resistance of Fe–Cr-based amorphous alloys, but this effect can be mitigated by the partial substitution of Fe by Si.

Moreover, the effect of replacing Fe with Si should be investigated on the corrosion resistance and GFA of Fe–Cr-based amorphous alloys containing Ni because the presence of Ni increases the Si content in SiO_2 passive films, making this film more protective.

The corrosion resistance should be analyzed under the conditions described in item a), and the results should be compared with those of 316 and 2205 stainless steel alloys, as shown in Section 4 to show promising behavior for use as reinforcements in reinforced concrete structures.

5.3. Effect of the partial replacement of Mo by Ni

As observed in Section 3.4, Mo addition, partially replacing Fe in Fe–Cr based amorphous alloys, has a more favorable effect on the GFA than the effect caused by Ni addition. However, considering corrosion resistance, Mo addition is unfavorable with the increase from neutral pH to an alkaline pH of 12. On the other hand, Ni addition does not impair corrosion resistance, when the neutral pH increases to an alkaline pH of 10 [74], as observed in Section 3.4. Ni addition shows better results when compared with Nb or Cu.

Given these findings, it is interesting to study the comparison between the effect of Ni and of Mo on the GFA and corrosion resistance of the Fe–Cr-based amorphous alloys in solutions of different pH values.

The effect of replacing Mo with Ni on the corrosion resistance and GFA of Fe–Cr-based amorphous alloys could also be interesting. The corrosion resistance should be analyzed under the conditions described in item a), and the results should be compared with those of 316 and 2205 stainless steel alloys.

5.4. Effect of partial crystallization on Fe–Cr-based amorphous alloys containing Si

As discussed above, the partial crystallization of Fe–Cr-based amorphous alloys decreases the corrosion resistance of the alloy mainly due to the formation of Cr- and Mo-depleted regions. Therefore, the dimensions of the part to be applied to explore the high corrosion resistance is limited by the GFA of the alloy composition. Nevertheless, as observed in Section 2, the partial crystallization of the amorphous Si content alloy promotes the formation of a SiO_2 passive film with a higher protective capacity. Therefore, the presence of a sufficiently high content of Si on the Fe–Cr-based amorphous alloys to form a SiO_2 passive film can be the way to mitigate the decrease in corrosion resistance caused by partial crystallization of the alloy.

Thus, it is worth studying the effect of partial crystallization on the corrosion resistance of BMG Fe–Cr-based containing Si.

5.5. Use of Fe–Cr–Si-based amorphous alloys as the anode in impressed current cathodic protection systems

Considering that a typical Fe–Si–Cr composition used as the anode in impressed current cathodic protection systems is crystalline

$\text{FeSi}_{14.5}\text{Cr}_{4.5}$, amorphous $\text{Fe}_x\text{Si}_{14.5}\text{Cr}_y$ alloys containing different Cr concentrations should be analyzed initially. Metalloids B should be added in an amount sufficient to enable the formation of a fully amorphous structure.

To analyze the performance of the anode, the anode consumption rate (kg/amp·year) of the $\text{Fe}_x\text{Si}_{14.5}\text{Cr}_y$ amorphous ribbon when used in the impressed current cathodic protection system of reinforced concrete structures should be determined. The results should be compared with the commercial anode $\text{FeSi}_{14.5}\text{Cr}_{4.5}$ or Ti (Ti/MMO) in an environment containing chloride.

References

- [1] C. Suryanarayana, A. Inoue, Iron-based bulk metallic glasses, *Int. Mater. Rev.* 58 (2013) 131–166.
- [2] A. Kobayashi, S. Yano, H. Kimura, A. Inoue, Mechanical property of Fe-base metallic glass coating formed by gas tunnel type plasma spraying, *Surf. Coat. Tech.* 202 (2008) 2513–2518.
- [3] S. Yoon, J. Kim, G. Bae, B. Kim, C. Lee, Formation of coating and tribological behavior of kinetic sprayed Fe-based bulk metallic glass, *J. Alloys Compd.* 509 (2011) 347–353.
- [4] D. Zenebe, S. Yi, S. Kim, Sliding friction and wear behavior of Fe-based bulk metallic glass in 3.5% NaCl solution, *J. Mater. Sci.* 47 (2012) 1446–1451.
- [5] C. Zhang, L. Liu, K.C. Chan, Q. Chen, C.Y. Tang, Wear behavior of HVOF-sprayed Fe-based amorphous coatings, *Intermetallics* 29 (2012) 80–85.
- [6] M.D. Archer, C.C. Corke, B.H. Harji, The electrochemical properties of metallic glasses, *Electrochim. Acta* 32 (1987) 13–26.
- [7] C.S. Kiminami, C.A.C. Souza, L.F. Bonavina, L.R.P. de Andrade Lima, S. Suriñach, M.D. Baró, C. Bolfarini, W.J. Botta, Partial crystallization and corrosion resistance of amorphous Fe–Cr–M–B (M = Mo, Nb) alloys, *J. Non-Cryst. Solids* 356 (2010) 2651–2657.
- [8] S.L. Wang, S. Yi, The corrosion behaviors of Fe-based bulk metallic glasses in a sulfuric solution at 70 degrees C, *Intermetallics* 18 (2010) 1950–1953.
- [9] S.L. Wang, H.X. Li, X.F. Zhang, S. Yi, Effects of Cr contents in Fe-based bulk metallic glasses on the glass forming ability and the corrosion resistance, *Mater. Chem. Phys.* 113 (2009) 878–883.
- [10] Z. Zhou, L. Wang, F.C. Wang, H.F. Zhang, Y.B. Liu, S.H. Xu, Formation and corrosion behavior of Fe-based amorphous metallic coatings by HVOF thermal spraying, *Surf. Coat. Technol.* 204 (2009) 563–570.
- [11] S.F. Guo, K.C. Chan, S.H. Xie, P. Yu, Y.J. Huang, H.J. Zhang, Novel centimeter-sized Fe-based bulk metallic glass with high corrosion resistance in simulated acid rain and seawater, *J. Non-Cryst. Solids* 369 (2013) 29–33.
- [12] H. Zohdi, H.R. Shahverdi, S.M.M. Hadavi, Effect of Nb addition on corrosion behavior of Fe-based metallic glasses in Ringer's solution for biomedical applications, *Electrochim. Commun.* 13 (2011) 840–843.
- [13] P.H. Tsai, A.C. Xiao, J.B. Li, J.S.C. Jang, J.P. Chu, J.C. Huang, Prominent Fe-based bulk amorphous steel alloy with large supercooled liquid region and superior corrosion resistance, *J. Alloys Compd.* 586 (2014) 94–98.
- [14] Y. Huang, G. Yuanzhi, F. Hongbo, S. Jun, Synthesis of Fe–Cr–Mo–C–B amorphous coating with high corrosion resistance, *Mater. Lett.* 89 (2012) 251–253.
- [15] Z.P. Lu, Y. Liu, C.T. Liu, M. Miller, P. Liaw, Evaluation of Glass-forming Ability in: Bulk Metallic Glasses, two ed. Springer Science, New York, 2008.
- [16] W. Guo, Y. Wu, J. Zhang, S. Hong, G. Li, G. Ying, J. Guo, Y. Qin, Fabrication and characterization of thermal-sprayed Fe-based amorphous/nanocrystalline composite coatings: an overview, *J. Therm. Spray Technol.* 23 (2014) 1157–1180.
- [17] L. Liu, C. Zhang, Fe-based amorphous coatings: structures and properties, *Thin Solid Films* 561 (2014) 70–86.
- [18] T. Masumoto, K. Hashimoto, M. Naka, Corrosion of amorphous alloys metals, *Proc. 3rd Int. Conf. on Rapidly Quenched Metals*, The Metals Society, London 1978, p. 435.
- [19] K. Hashimoto, M. Naka, K. Asami, T. Masumoto, The role of alloying elements in improving the corrosion resistance of amorphous iron base alloys, *Corros. Sci.* 19 (1979) 857–867.
- [20] C. Suryanarayana, A. Inoue, *Bulk Metallic Glasses*, first ed. CRC. Press, Boca Raton FL, 2011.
- [21] M.J. Duarte, J. Klemm, S.O. Klemm, K.J.J. Mayrhofer, M. Stratmann, S. Borodin, A.H. Romero, M. Madinehei, D. Crespo, J. Serrano, S.S.A. Gerstl, P.P. Choi, D. Raabe, F.U. Renner, Element-resolved corrosion analysis of stainless-type glass-forming steels, *Science* 341 (2013) 372–376.
- [22] M. Belkhaouda, L. Bazzia, A. Benlhemib, R. Salghic, B. Hammoutid, S. Kertite, Effect of the heat treatment on the corrosion behaviour of amorphous Fe–Cr–P–C–Si alloy in 0.5 M H_2SO_4 , *Appl. Surf. Sci.* 252 (2006) 7921–7925.
- [23] S.M. Gravano, S. Torchio, E. Angelini, C. Antonino, M. Baricco, Structural aspects and the anodic behavior of $\text{Fe}_{34}\text{Ni}_{36}\text{Cr}_{10}\text{P}_{14}\text{B}_6$ amorphous alloy submitted to different heat treatments, *Corros. Sci.* 32 (1991) 509–519.
- [24] I. Chatteraj, S. Baunack, M. Stoica, A. Gebert, Electrochemical response of $\text{Fe}_{65.5}\text{Cr}_4\text{Mo}_4\text{Ga}_4\text{P}_{12}\text{C}_5\text{B}_{5.5}$ bulk amorphous alloy in different aqueous media, *Mater. Corros.* 55 (2004) 36–42.
- [25] F.F. Marzo, A.R. Pierna, M.M. Vega, Effect of irreversible structural relaxation on the electrochemical behavior of $\text{Fe}_{78-x}\text{Si}_{13}\text{B}_9\text{Cr}_{(x=3,4,7)}$ amorphous alloys, *J. Non-Cryst. Solids* 329 (2003) 108–114.

- [26] H. Habazaki, A. Kawashima, K. Asami, K. Hashimoto, The effect of structural relaxation on the passivation behavior of amorphous Fe-Cr-W-P-C alloys, *Corros. Sci.* 31 (1990) 343–348.
- [27] L. Gong, H. Lei, D.Y. Guo, H.G. Wei, Q. Li, J. Qin, M.M. Zhen, L.R. Ping, Corrosion behavior of bulk metallic glasses in different aqueous solutions, *Sci. China Phys. Mech. Astron.* 53 (2010) 435–439.
- [28] R. Raicheff, V. Zaprianova, E. Gattef, Effect of structural relaxation on electrochemical corrosion behavior of amorphous alloys, *J. Mater. Sci. Lett.* 16 (1997) 1701–1704.
- [29] J. Shen, Q.J. Chen, J.F. Sun, H.B. Fan, G. Wang, Exceptionally high glass-forming ability of an FeCoCrMoCBy alloy, *Appl. Phys. Lett.* 86 (2005) 151907–1–151907–3.
- [30] D. Zander, U. Koster, Corrosion of amorphous and nanocrystalline Zr-based alloys, *Mater. Sci. Eng. A* 375 (2004) 53–59.
- [31] C.A.C. Souza, C. Kiminami, Crystallization and corrosion resistance of amorphous FeCuNbSiB, *J. Non-Cryst. Solids* 219 (1997) 155–159.
- [32] D. Szewieczek, A. Baron, Electrochemical corrosion and its influence on magnetic properties of Fe_{75.5}Si_{13.5}B₉Nb₃Cu₁ alloy, *J. Mater. Process. Technol.* 164 (2005) 940–946.
- [33] C.A.C. Souza, S.E. Kuri, F.S. Politi, J.E. May, C.S. Kiminami, Corrosion resistance of amorphous and polycrystalline FeCuNbSiB alloys in sulphuric acid solution, *J. Non-Cryst. Solids* 247 (1999) 69–73.
- [34] H.Y. Tong, F.G. Shi, J. Lavernia, Enhanced oxidation resistance of nanocrystalline FeBSi materials, *Scripta Metall. Mater.* 32 (1995) 511–516.
- [35] M.J. Duarte, A. Kostka, J.A. Jimenez, P. Choi, J. Klemm, D. Crespo, D. Raabe, F.U. Renner, Crystallization, phase evolution and corrosion of Fe-based metallic glasses: an atomic-scale structural and chemical characterization study, *Acta Mater.* 71 (2014) 20–30.
- [36] H.X. Li, S. Yi, Corrosion behaviors of bulk metallic glasses Fe_{66.7}Cr_{7.0}Si_{3.3}B_{5.5}P_{8.7}Cr_{2.3}Al_{2.0}Mo_{4.5} having different crystal volume fractions, *Mater. Chem. Phys.* 112 (2008) 305–309.
- [37] H.M. Ha, J.H. Payer, Devitrification of Fe-based amorphous metal SAM 1651: a structural and compositional study, *Metall. Mater. Trans. A* 40 (2009) 2519–2529.
- [38] Y. Yang, C. Zhang, Y. Peng, Y. Yu, L. Liu, Effects of crystallization on the corrosion resistance of Fe-based amorphous coatings, *Corros. Sci.* 59 (2012) 10–19.
- [39] J. Farmer, J.S. Choi, C. Saw, J. Haslam, D. Day, P. Hailey, T. Lian, R. Rebak, J. Perepezko, J. Payer, D. Branagan, B. Beardsley, A. D'Amato, L. Aprigliano, Iron-based amorphous metals: high-performance corrosion-resistant material development, *Metall. Mater. Trans. A* 40A (2009) 1289–1305.
- [40] L. Liu, C. Zhang, Fe-based amorphous coatings: structures and properties, *Thin Solid Films* 561 (2014) 70–86.
- [41] G.Y. Koga, R.P. Nogueira, V. Roche, A.R. Yavari, A.K. Melle, J. Gallego, C. Bolfarini, C.S. Kiminami, W.J. Botta, Corrosion properties of Fe-Cr-Nb-B amorphous alloys and coatings, *Surf. Coat. Technol.* 254 (2014) 238–243.
- [42] M.D. Archer, C.C. Corke, B.H. Harji, The electrochemical properties of metallic glasses, *Electrochim. Acta* 32 (1987) 13–26.
- [43] S.J. Pang, T. Zhang, K. Asami, A. Inoue, Bulk glassy Fe-Cr-Mo-C-B alloys with high corrosion resistance, *Corros. Sci.* 44 (2002) 1847–1856.
- [44] P.F. Gostin, S. Oswald, L. Schultz, A. Geber, Acid corrosion process of Fe-based bulk metallic glass, *Corros. Sci.* 62 (2012) 112–121.
- [45] S.J. Pang, T. Zhang, K. Asami, A. Inoue, Synthesis of Fe-Cr-Mo-C-B-P bulk metallic glasses with high corrosion resistance, *Acta Mater.* 50 (2002) 489–497.
- [46] R.Q. Guo, C. Zhang, Y. Yang, Y. Peng, L. Liu, Corrosion and wear resistance of a Fe-based amorphous coating in underground environment, *Intermetallics* 30 (2012) 94–99.
- [47] B. Movahedi, M. Enayati, C. Wong, Structural and thermal behavior of Fe-Cr-Mo-P-B-C-Si amorphous and nanocrystalline HVOF coatings, *J. Therm. Spray Technol.* 19 (2010) 1093–1099.
- [48] M.F. López, M.L. Escudero, E. Vida, A.R. Pierna, Corrosion behaviour of amorphous Fe Cr Ni (Si,P) alloys, *Electrochim. Acta* 42 (1997) 659–665.
- [49] C.A.C. Souza, C. Bolfarini, F.W.J. Botta, L.R.P. de Andrade Lma, M.F. de Oliveira, C.S. Kiminami, Corrosion resistance and glass forming ability of Fe₄₇Co₇Cr₁₅M₉Si₅B₁₅Y₂(M=Mo, Nb) amorphous alloys, *Mater. Res.* 16 (2013) 1–5 (São Carlos).
- [50] S.L. Wang, H.X. Li, X.F. Zhang, S. Yi, Effects of Cr contents in Fe-based bulk metallic glasses on the glass forming ability and the corrosion resistance, *Mater. Chem. Phys.* 113 (2009) 878–883.
- [51] L. Hongxiang, Y. Siwei, Corrosion behaviors of bulk metallic glasses Fe_{66.7}Cr_{7.0}Si_{3.3}B_{5.5}P_{8.7}Cr_{2.3}Al_{2.0}Mo_{4.5} having different crystal volume fractions, *Mater. Chem. Phys.* 112 (2008) 305–309.
- [52] Z.C. Zhang, Z.L. Clong, J. Peng, H.Q. Wei, P. Tang, X.G. Li, Preparation and properties of Fe-Co-B-Si-Nb-Cr soft-magnetic bulk amorphous alloys, *Rare Metal Mater. Eng.* 39 (2010) 162–168.
- [53] M. Haijian, W. Weimin, Z. Jie, Z. Hongdi, Ma.L. Guihua, C. Chongde, Crystallization and corrosion resistance of (Fe_{0.78}Si_{0.09}B_{0.13})_{100-x}Ni_x (x = 0, 2 and 5) glassy alloys, *J. Mater. Sci. Technol.* 27 (2011) 1169–1177.
- [54] M.F. Lopez, M.L. Escudero, E. Vida, The corrosion resistance can be improved by an addition of Si element in the Fe-Cr-Ni alloy, *Electrochim. Acta* 42 (1997) 659–665.
- [55] J. Jayaraj, K.B. Kim, H.S. Ahn, E. Fleury, Corrosion mechanism of N-containing Fe-Cr-Mo-YC-B bulk amorphous alloys in highly concentrated HCl solution, *Mater. Sci. Eng. A* 449 (2007) 517–520.
- [56] Z.B. Zheng, Y.G. Zheng, W.H. Sun, J.Q. Wang, Effect of applied potential on passivation and erosion-corrosion of a Fe-based amorphous metallic coating under slurry impingement, *Corros. Sci.* 82 (2014) 115–124.
- [57] M.S. Bakare, K.T. Voisey, K. Chokethawai, D.G. McCartney, Corrosion behaviour of crystalline and amorphous forms of the glass forming alloy Fe₄₃Cr₁₆Mo₁₆C₁₅B₁₀, *J. Alloys Compd.* 527 (2012) 210–218.
- [58] F. Otsubo, H. Era, K. Kishitake, Formation of amorphous Fe-Cr-Mo-8P-2C coatings by the high velocity oxy-fuel process, *J. Therm. Spray Technol.* 9 (2000) 494–498.
- [59] H.S. Ni, X.H. Liu, X.C. Chang, W.L. Hou, W. Liu, J.Q. Wang, High performance amorphous steel coating prepared by HVOF thermal spraying, *J. Alloys Compd.* 467 (2009) 163–167.
- [60] M.W. Tan, E. Akiyama, H. Habazaki, A. Kawashima, K. Asami, K. Hashimoto, The role of chromium and molybdenum in passivation of amorphous Fe-Cr-Mo-P-C alloys in deaerated 1 M HCl, *Corros. Sci.* 38 (1996) 2137–2151.
- [61] M.W. Tan, E. Akiyama, A. Kawashima, K. Asami, K. Hashimoto, The effect of air exposure on the corrosion behavior of amorphous Fe-8Cr-Mo-13P-7C alloys in 1 M HCl, *Corros. Sci.* 37 (1995) 1289–1301.
- [62] P.F. Gostin, A. Gebert, L. Schultz, Comparison of the corrosion of bulk amorphous steel with conventional steel, *Corros. Sci.* 52 (2010) 273–281.
- [63] M.W. Tan, E. Akiyama, H. Habazaki, A. Kawashima, K. Asami, K. Hashimoto, The role of chromium and molybdenum in passivation of amorphous Fe-Cr-Mo-PC alloys in deaerated 1 M HCl, *Corros. Sci.* 38 (1996) 2137–2154.
- [64] M. Liqun, A. Inoue, On glass-forming ability of Fe-based amorphous alloys, *Mater. Lett.* 38 (1999) 58–61.
- [65] A. Inoue, A. Takeuchi, Mixing enthalpy of liquid phase calculated by miedema's scheme and approximated with sub-regular solution model for assessing forming ability of amorphous and glassy alloys, *Intermetallics* 18 (2010) 1779–1789.
- [66] J. Blink, J. Farmer, J. Choi, C. Saw, Applications in the nuclear industry for thermal spray amorphous metal and ceramic coatings, *Metall. Mater. Trans. A* 40 (2009) 1344–1354.
- [67] Z.P. Lu, C.T. Liu, W.D. Porter, Role of yttrium in glass formation of Fe based bulk metallic glasses, *Appl. Phys. Lett.* 83 (2003) 2581–2583.
- [68] J.C. Farmer, J.S. Choi, C.K. Saw, R.H. Rebak, S.D. Day, T. Lian, P.D. Hailey, J.H. Payer, D.J. Branagan, L.F. Aprigliano, Corrosion resistance of amorphous Fe_{49.7}Cr_{17.7}Mn_{1.9}Mo_{7.4}W_{1.6}B_{15.2}C_{3.8}Si_{2.4}, *J. Nucl. Technol.* 161 (2008) 169–189.
- [69] J. Jayaraj, K.B. Kim, H.S. Ahn, E. Fleury, Corrosion mechanism of N-containing Fe-Cr-Mo-YC-B bulk amorphous alloys in highly concentrated HCl solution, *Mater. Sci. Eng. A* 449 (2007) 517–520.
- [70] J.T. Kim, S.H. Hong, C.H. Lee, J.M. Park, T.W. Kim, W.H. Lee, H.I. Yim, K.B. Kim, Plastic deformation behavior of Fe-Co-B-Si-Nb-Cr bulk metallic glasses under nanoindentation, *J. Alloys Compd.* 587 (2014) 415–419.
- [71] Z.L. Long, Y. Shao, X.H. Deng, Z.C. Zhang, Y. Jiang, P. Zhang, B.L. Shen, A. Inoue, Cr effects on magnetic and corrosion properties of Fe-Co-Si-B-N-Nb bulk glassy alloys with high glass-forming ability, *Intermetallics* 15 (2007) 1453–1458.
- [72] H. Matsumoto, A. Urata, Y. Yamada, A. Inoue, Novel Fe (97-x-y)PxB₂Cr₁ alloys with high magnetization and low loss characteristics for inductor core materials, *IEEE Trans. Magn.* 46 (2010) 373–376.
- [73] H. Zohdi, H.R. Shahverdi, S.M.M. Hadavi, Effect of Nb addition on corrosion behavior of Fe-based metallic glasses in Ringer's solution for biomedical applications, *Electrochem. Commun.* 13 (2011) 840–843.
- [74] W.J. Botta, J.E. Berger, C.S. Kiminami, V. Roche, R.P. Nogueira, C. Bolfarini, Corrosion resistance of Fe-based amorphous alloys, *J. Alloys Compd.* 586 (2014) S105–S110.
- [75] S.J. Pang, T. Zhang, K. Asami, A. Inoue, New Fe-Cr-MO-(Nb,Ta)C-B glassy alloys with high glass-forming ability and good corrosion resistance, *Mater. Trans. JIM.* 42 (2001) 376–379.
- [76] C.A.C. Souza, J.E. May, M.F. de Oliveira, S.E. Kuri, C.S. Kiminami, I.A. Carlos, Influence of the corrosion on the saturation magnetic density of amorphous and nanocrystalline Fe₇₃Nb₅Si_{15.5}B_{7.5}Cu₁ and Fe₈₀Zr_{13.5}Nb_{3.5}B₁₂Cu₁ alloys, *J. Non-Cryst. Solids* 304 (2002) 210–216.
- [77] F. Zhai, E. Pineda, M.J. Duarte, D. Crespo, Role of Nb in glass formation of Fe-Cr-Mo-C-B-Nb BMGs, *J. Alloys Compd.* 604 (2014) 157–163.
- [78] C.T. Chang, Y.H. Ding, Y. Shao, P. Zhang, B.L. Shen, A. Inoue, Corrosion behavior of Fe-based ferromagnetic (Fe, Ni)-B-Si-Nb bulk glassy alloys in aqueous electrolytes, *J. Non-Cryst. Solids* 354 (2008) 4609–4613.
- [79] W.J. Botta, J.E. Berger, C.S. Kiminami, V. Roche, R.P. Nogueira, C. Bolfarini, Corrosion resistance of Fe-based amorphous alloys, *J. Alloys Compd.* 586 (2014) 105–110.
- [80] J.H. Guo, Z. Gao, X.J. Ni, D.R. Li, Z.C. Lu, Electrochemical behavior of bulk amorphous steel Fe₅₅M₂Cr₁₂Mo₁₀B₆C₁₃Y₂ (M= Ni, Cu, Nb), *J. Iron Steel Res. Int.* 17 (2010) 69–73.
- [81] L. Yanhui, J. Xingjie, Z. Wei, F. Canfeng, W. Xuewei, Q. Fengxiang, Y. Shinichi, Y. Yoshihiko, Effects of alloying elements on the thermal stability and corrosion resistance of an Fe-based metallic glass with low glass transition temperature, *Metall. Mater. Trans. A* 45 (2014) 2393–2398.
- [82] L. Xue, H. Kato, X. Li, H. Kato, K. Yubuta, A. Makino, A. Inoue, Improved plasticity of iron-based high-strength bulk metallic glasses by copper-induced nanocrystallization, *J. Non-Cryst. Solids* 357 (2011) 3002–3005.
- [83] P.H. Tsai, A.C. Xiao, J.B. Li, J.S.C. Jang, J.P. Chu, J.C. Huang, Prominent Fe-based bulk amorphous steel alloy with large supercooled liquid region and superior corrosion resistance, *J. Alloys Compd.* 586 (2014) 94–98.
- [84] A. Inoue, B.L. Shen, C.T. Chang, Super-high strength of over 4000 MPa for Fe-based bulk glassy alloys in [(Fe_{1-x}Co_x)_{0.75}Bo_{2.5}Si_{0.05}Nb₄] system, *Acta Mater.* 52 (2004) 4093–4099.
- [85] X.J. Gu, S.J. Poon, G.J. Shiflet, Effects of carbon content on the mechanical properties of amorphous steel alloys, *Scr. Mater.* 57 (2007) 289–292.
- [86] H.Z. Fang, X.D. Hui, G.L. Chen, Effects of Mn addition on the magnetic property and corrosion resistance of bulk amorphous steels, *J. Alloys Compd.* 464 (2008) 292–295.
- [87] Y.B. Wang, H.F. Li, Y.F. Zheng, M. Li, Corrosion performances in simulated body metallic glasses, *Mater. Sci. Eng. C* 32 (2012) 599–606.

- [88] S.F. Guo, K.C. Chan, S.H. Xie, P. Yu, Y.J. Huang, H.J. Zhang, Novel centimeter-sized Fe-based bulk metallic glass with high corrosion resistance in simulated acid rain and seawater, *J. Non-Cryst. Solids* 369 (2013) 29–33.
- [89] G.C. Lavorato, G. Fiore, A. Castellero, M. Baricco, J.A. Moya, Preparation and characterization of Fe-based bulk metallic glasses in plate form, *Phys. Rev. B Condens. Matter* 407 (2012) 3192–3195.
- [90] G.Y. Koga, R.P. Nogueira, V. Roche, A.R. Yavari, A.K. Melle, J. Gallego, C. Bolfarini, C.S. Kiminami, W.J. Botta, Corrosion properties of Fe–Cr–Nb–B amorphous alloys and coatings, *Surf. Coat. Technol.* 254 (2014) 238–243.
- [91] F. Otsubo, K. Kishitake, Corrosion resistance of Fe–16%Cr–30%Mo–(C,B,P) amorphous coatings sprayed by HVOF and APS processes, *Mater. Trans. JIM* 46 (2005) 80–83.
- [92] A. Kobayashi, S. Yano, H.M. Kimura, A. Inoue, Fe-based metallic glass coatings produced by smart plasma spraying process, *Mater. Sci. Eng. B* 148 (2008) 110–113.
- [93] J. Blink, J. Farmer, J. Choi, C. Saw, Applications in the nuclear industry for thermal spray amorphous metal and ceramic coatings, *Metall. Mater. Trans. A* 40 (2009) 1344–1358.
- [94] Y. Wang, Y.G. Zheng, W. Ke, W.H. Sun, W.L. Hou, X.C. Chang, J.Q. Wang, Slurry erosion–corrosion behavior of high-velocity oxy-fuel (HVOF) sprayed Fe-based amorphous metallic coatings for marine pump in sand-containing NaCl solutions, *Corros. Sci.* 53 (2011) 3177–3185.
- [95] J. Lin, Z. Wang, P. Lin, J. Cheng, X. Zhang, S. Hong, Microstructure and cavitation erosion behavior of FeNiCrBSiNbW coating prepared by twin wires arc spraying process, *Surf. Coat. Technol.* 240 (2014) 432–436.
- [96] A.H. Tuthill, C.M. Schillmoller, *Ocean Sci. and Ocean Eng. Conf.*, INCO Tech. Pub. A404, Marine Technology Society, Washington, DC, 1965.
- [97] A. Scrivani, S. Ianelli, A. Rossi, R. Groppetti, F. Casadei, G. Rizzi, A contribution to the surface analysis and characterisation of HVOF coatings for petrochemical application, *Wear* 250 (2001) 107–113.
- [98] J. Koutsky, High velocity oxy-fuel spraying, *J. Mater. Process. Technol.* 157–158 (2004) 557–560.
- [99] D.V. Val, M.G. Stewart, Life-cycle cost analysis of reinforced concrete structures in marine environments, *Struct. Safety* 25 (2003) 343–362.
- [100] A.C. Dutra, L. De Paula Nunes, *Proteção Catódica – Técnica de combate à corrosão*, fifth ed. Interciência, Rio de Janeiro, 2011.
- [101] I. Gurrappa, I. Yashwanth, I. Mounika, Cathodic protection technology of naval structures against corrosion, *Proc. Natl. Acad. Sci., India, Sect. A* 85 (2015) 1–18.
- [102] O. Jin-Seok, K. Jong-Do, A new protection strategy of impressed current cathodic protection for ship, *KSME Int. J.* 18 (2004) 592–596.
- [103] D.V. Ribeiro, A. Sales, C.A.C. Souza, F.C.R. Almeida, M.P.T. Cunha, M.Z. Lourenço, P. Helene, *Corrosão em armadura de concreto armado*, fifth ed. Elsevier, Rio de Janeiro, 2013.